# Io's Atmospheric Response to Eclipse: UV Aurorae Observations

K. D. Retherford, *et al.*

*Science* **318**, 237 (2007);
DOI: 10.1126/science.1147594

that the troughs are a truly global phenomenon. No trough was seen near longitude 270°W, but that region is geologically complex, with numerous crisscrossing dark lineaments. The north-south offset of the antipodal centers of symmetry, maintained in the New Horizons images, hints at true polar wander of Europa's ice shell (*21–23*).

From Earth, the solar phase angle *g* for the Jupiter system is ≤12°, limiting Earth-based measurement of directional scattering by jovian satellites. Only spacecraft can access higher phase angles. LORRI observed the Galilean satellites at a range of phase angles (table S1), filling gaps in Europa's solar phase curve between 32° and 103° and between 109° and 143°. The photometric data, corrected for longitudinal variations and normalized to Voyager data (*24*), are shown in Fig. 4. Europa's brightness at $g$ = 70° is more than 40% of its fully illuminated brightness, underscoring the unique texture of its surface produced by active resurfacing. The comparable number for Earth's Moon is only 20%.

Our observations improve measurement of Europa's phase integral *q*, which describes the directional scattering properties of light reflected from its surface. The new *q* value is 1.01 ± 0.04, compared with 1.1 ± 0.1 from previous Voyager data (*24*). Compared with other actively resurfaced icy satellites, Europa's *q* is marginally higher than that of Enceladus (0.89 ± 0.10) (*25*) but lower than that of Triton (1.14 ± 0.03) (*26*). Using a geometric albedo of 0.67 ± 0.03 for LORRI wavelengths (*8*, *24*), we find a new Bond albedo of 0.68 ± 0.05, compared with a previous value of 0.6 ± 0.1 (*24*), meaning that Europa absorbs less sunlight than previously thought.

### References and Notes


1. T. V. Johnson, C. M. Yeats, R. Young, *Space Sci. Rev.* **60**, 3 (1992).
2. F. Bagenal, T. E. Dowling, W. B. McKinnon, Eds., *Jupiter: The Planet, Satellites, and Magnetosphere* (Cambridge Univ. Press, New York, 2004).
3. T. B. McCord *et al.*, *Science* **280**, 1242 (1998).
4. T. B. McCord *et al.*, *J. Geophys. Res.* **104**, 11827 (1999).
5. T. B. McCord, G. B. Hansen, C. A. Hibbitts, *Science* **292**, 1523 (2001).
6. S. A. Stern, *Space Sci. Rev.*, in press; preprint available at http://arxiv.org/abs/0709.4417.
7. D. C. Reuter *et al.*, *Space Sci. Rev.*, in press; preprint available at http://arxiv.org/abs/0709.4281.
8. A. F. Cheng *et al.*, *Space Sci. Rev.*, in press; preprint available at http://arxiv.org/abs/0709.4278.
9. F. P. Fanale *et al.*, *J. Geophys. Res.* **106**, 14595 (2001).
10. K. P. Hand, C. F. Chyba, *Icarus* **189**, 424 (2007).
11. R. W. Carlson, R. E. Johnson, M. S. Anderson, *Science* **286**, 97 (1999).
12. R. W. Carlson, M. S. Anderson, R. E. Johnson, M. B. Schulman, A. H. Yavrouian, *Icarus* **157**, 456 (2002).
13. R. W. Carlson, M. S. Anderson, R. Mehlman, R. E. Johnson, *Icarus* **177**, 461 (2005).
14. J. B. Dalton *et al.*, *Icarus* **177**, 472 (2005).
15. R. E. Johnson *et al.*, in *Jupiter: The Planet, Satellites, and Magnetosphere*, F. Bagenal, T. E. Dowling, W. B. McKinnon, Eds. (Cambridge Univ. Press, New York, 2004), pp. 485–512.
16. A. S. McEwen, *J. Geophys. Res.* **91**, 8077 (1986).
17. W. M. Grundy, B. Schmitt, *J. Geophys. Res.* **103**, 25809 (1998).
18. P. M. Schenk, C. R. Chapman, K. Zahnle, J. M. Moore, in *Jupiter: The Planet, Satellites, and Magnetosphere*, F. Bagenal, T. E. Dowling, W. B. McKinnon, Eds. (Cambridge Univ. Press, New York, 2004), pp. 427–456.
19. P. M. Schenk, *Lunar Planet. Sci. Conf.* **36**, 2081 (2005).
20. R. Greeley *et al.*, in *Jupiter: The Planet, Satellites, and Magnetosphere*, F. Bagenal, T. E. Dowling, W. B. McKinnon, Eds. (Cambridge Univ. Press, New York, 2004), pp. 329–362.
21. A. C. Leith, W. B. McKinnon, *Icarus* **120**, 387 (1996).
22. A. R. Sarid *et al.*, *Icarus* **158**, 24 (2002).
23. P. M. Schenk, I. Matsuyama, F. Nimmo, Lunar and Planetary Institute's "Ices, Oceans, and Fire: Satellites of the Outer Solar System" meeting, Boulder CO, 3 to 15 August 2007, abstract 6090 (2007); available at www.lpi.usra.edu/meetings/icysat2007/pdf/6090.pdf.
24. B. J. Buratti, J. Veverka, *Icarus* **55**, 93 (1983).
25. B. J. Buratti, J. Veverka, *Icarus* **58**, 254 (1984).
26. J. Hillier *et al.*, *Science* **250**, 419 (1990).
27. G. B. Hansen, T. B. McCord, *J. Geophys. Res.* **109**, E01012 (2004).


28. We thank the entire New Horizons mission team and our colleagues on the New Horizons science team. New Horizons is funded by NASA, whose financial support we gratefully acknowledge. We also thank C. A. Hibbits, J. B. Dalton III, G. B. Hansen, and K. Stephan for valuable scientific discussions as well as providing examples of NIMS data.


### Supporting Online Material

www.sciencemag.org/cgi/content/full/318/5848/234/DC1
Table S1


10 July 2007; accepted 21 September 2007
10.1126/science.1147623


REPORT

# Io's Atmospheric Response to Eclipse: UV Aurorae Observations


K. D. Retherford,[1*] J. R. Spencer,[2] S. A. Stern,[3] J. Saur,[4] D. F. Strobel,[5] A. J. Steffl,[2] G. R. Gladstone,[1] H. A. Weaver,[6] A. F. Cheng,[3] J. Wm. Parker,[2] D. C. Slater,[1] M. H. Versteeg,[1] M. W. Davis,[1] F. Bagenal,[7] H. B. Throop,[2] R. M. C. Lopes,[8] D. C. Reuter,[9] A. Lunsford,[9] S. J. Conard,[6] L. A. Young,[2] J. M. Moore[10]



**The New Horizons (NH) spacecraft observed Io's aurora in eclipse on four occasions during spring 2007. NH Alice ultraviolet spectroscopy and concurrent Hubble Space Telescope ultraviolet imaging in eclipse investigate the relative contribution of volcanoes to Io's atmosphere and its interaction with Jupiter's magnetosphere. Auroral brightness and morphology variations after eclipse ingress and egress reveal changes in the relative contribution of sublimation and volcanic sources to the atmosphere. Brightnesses viewed at different geometries are best explained by a dramatic difference between the dayside and nightside atmospheric density. Far-ultraviolet aurora morphology reveals the influence of plumes on Io's electrodynamic interaction with Jupiter's magnetosphere. Comparisons to detailed simulations of Io's aurora indicate that volcanoes supply 1 to 3% of the dayside atmosphere.**


Io is a volcanically active moon of Jupiter, and its volcanism is the ultimate source of material for Io's sulfur-dioxide atmosphere. The interaction between Io's atmosphere and the Io plasma torus produces displays of auroral emissions on Io, supplies plasma to Jupiter's magnetosphere, and physically links Io to Jupiter (*1*). The relative importance of the volcanoes as a direct, immediate source of the atmosphere, versus sublimation of frosts deposited around these volcanoes, has remained uncertain since the atmosphere's discovery in 1979 (*2*, *3*). Io's average dayside surface temperature rapidly drops after eclipse ingress or at night [likely from ~120 K to ~90 K; (*4*, *5*)], which is sufficient to diminish the sublimation component of the atmosphere across most of the surface and possibly results in an atmosphere mostly supplied directly from volcanoes.

Aurora observations, particularly while Io is in solar eclipse by Jupiter, can provide information on both Io's atmosphere and its interaction with Jupiter (*6–14*). The New Horizons (NH) spacecraft was able to observe Io in eclipse four times during its flyby of Jupiter in late February and early March 2007 (Table 1).

We report NH Alice ultraviolet (UV) spectrometer (*15*) observations of Io eclipse ingress and egress. Io eclipse observations by other NH instruments are reported separately (*16*, *17*). Alice provides spectral images in the extreme- and far-UV (EUV and FUV) pass-bands from 52 nm to 187 nm with 0.3- to 0.4-nm resolution for point sources and 1.0- to 1.2-nm resolution for extended sources, as Io was for our observations (*18*), and a spatial resolution of 0.1° by 0.3° along the 4° long narrow part of its slit.

Supporting observations were also made with the Advanced Camera for Surveys Solar Blind Channel (ACS/SBC) (*19*) on the Hubble Space Telescope (HST). Angular plate scales of 0.034 arc sec/pixel and 0.030 arc sec/pixel on the detector result in slightly rectangular pixels. Use of the SBC's F125LP filter excludes sky background signal from geocoronal Lyman-α emissions while passing through the atomic oxygen (OI) 130.4 nm and longer FUV emissions of interest for Io.

Auroral emission features include a global limb glow around the disk of the satellite, sub-Jupiter and anti-Jupiter equatorial spots (or glows), and a wake region (on the orbital leading hemisphere, downstream relative to the magnetospheric plasma flow). These large-scale features are known to change brightness and location with Jupiter's changing magnetic field orientation at Io and are diagnostic of the local flow of the Io plasma torus past the satellite and into its atmosphere (*10*, *11*, *20*–*23*). Dramatic visible auroral glows have been seen from numerous volcanic plumes, including the large Tvashtar plume that was active at this time (*17*).

The question of how much of the dayside atmosphere comes from $SO_2$ frost sublimation versus volcanoes remains difficult to resolve. Previous theoretical work demonstrated that auroral brightness variations with time after Io enters eclipse ingress provide a means to investigate the relative contributions of volcanic and sublimation sources to Io's dayside atmosphere (*14*). A relative contribution from volcanoes of 1 to 10% was suggested based on only a few data points with inadequate time coverage.

We observed the time series of Io's FUV emissions in shadow using Alice (Fig. 1) and the HST/SBC (Fig. 2). The last Alice exposure in IEclipse05 (red points in Fig. 3, A to C) is ~40% brighter than it is in earlier measurements (Table 2) and likely represents predicted posteclipse aurora brightening (*14*). In IEclipse01, the view is of the dayside, similar to that for HST (Fig. 2). This view includes Io's wake emissions. The high initial brightnesses and the decrease in brightness after ingress in IEclipse01 (Fig. 3) may be because the amount of sublimation is particularly sensitive to changes after eclipse ingress on the dayside atmosphere. There was little change in volcanic activity observed during the encounter period (*17*); thus, any changes in Io's neutral atmospheric density must be attributed to other sources. The plasma torus density is thought to be relatively stable on the time scale of days. The trend of brighter aurora with Io's location in denser regions of the plasma torus (*21*) would exacerbate the difference in measured OI 135.6-nm brightnesses between IEclipse01 and IEclipse04 (fig. S1B). Viewing geometry of the asymmetric atmosphere regions and the large-scale auroral features viewed (e.g., wake viewed in IEclipse01 but not IEclipse04) could explain the differences, but the FUV equatorial spots are consistently brighter than the wake so the IEclipse04 view is favored. Also, measurements of $SO_2$ longitudinal distribution (*24*) suggest that the dayside equatorial densities in the region viewed in IEclipse01 (at 344°) are a few times less dense than IEclipse04 (at 241°). The two Alice ingress series are best explained by a dramatic difference between the densities of Io's dayside and nightside atmospheres.

The HST/SBC data (Fig. 3D) show that Io's FUV brightness decreased between the first and last exposures by roughly factors of 1.5 and 1.3 for square regions of widths 0.55 $R_{Io}$ and 4 $R_{Io}$ (Io radii), respectively, centered on Io. The most prominent FUV emission lines that contribute to this image are the same neutral OI 130.4 nm, OI 135.6 nm, and SI 147.9 nm lines observed with Alice (Fig. 1B). However, the first SBC exposure occurred 12 min after umbral ingress, which is after the time expected for the most dramatic variations. Alice observed the key periods for IEclipse01 and IEclipse04, but only two points at ~90 min after ingress for this IEclipse03 event. Cassini visible aurora imaging (*11*) showed similarly moderate variations in brightness over a period starting ~20 min after ingress.

A comparison between aurora simulations and the auroral brightness time series shown in Fig. 3 enables a higher fidelity assessment of Io's atmospheric sources. Volcanic column densities of $2 \times 10^{14}$ cm$^{-2}$, $4 \times 10^{14}$ cm$^{-2}$, and $8 \times 10^{14}$ cm$^{-2}$ out of $1.5 \times 10^{16}$ cm$^{-2}$ were used in Fig. 3 (1%, 3%, and 5% cases, respectively). The data are best described by a volcanic contribution of 1 to 3% to a primarily sublimation-supplied dayside atmosphere. Volcanic contributions of >5% are rejected for the epoch of these observations.

Other methods for characterizing the atmospheric sources face the predicament of collocated volcanic plumes and $SO_2$ frost deposits, potentially confusing spatial associations of higher density near volcanoes with the respective sources. Recent reports using these other methods are in general agreement with the results of 1 to 3% reported here (*25*, *26*), but $SO_2$ maps derived from Lyman-α absorption images show more gas near the equatorial terminators than expected (*27*, *28*, *24*) and remain difficult to reconcile with these levels of sublimation.

The latitudinal extent of the sub-Jupiter equatorial spot (Fig. 2, C to F) decreased by ~25% from 17 to 37 min after umbral ingress. Space Telescope Imaging Spectrograph (STIS) Io eclipse observations similarly hinted at FUV emissions more localized to the magnetic equator (*13*). In shadow, preferential closure of Io's electrodynamic current system was predicted to occur through local plume atmospheres (*29*, *30*). A combination of local dominance of the plume atmosphere over the sublimation source could explain this variation in the latitudinal extent of the sub-Jupiter equatorial spot with time in eclipse.

An emission feature between 200 km and 550 km above the limb and located near the bright, newly discovered "East Girru" volcano is seen in

**Table 1.** NH Io eclipse Alice observation summary. Supporting observations with the HST/SBC are also indicated. IEclipse02 was dropped from the plan and not performed.

| Visit name | Date | Umbral ingress | Umbral egress | Instrument used | Number of exposures |
|---|---|---|---|---|---|
| IEclipse01 | 2/25/2007 | 19:53 | 21:58 | Alice | 16 |
| IEclipse03 | 2/27/2007 | 14:21 | 16:27 | Alice | 2 |
| | | | | HST/SBC | 8 |
| IEclipse04 | 3/1/2007 | 8:50 | 10:56 | Alice | 20 |
| IEclipse05 | 3/3/2007 | 3:18 | 5:25 | Alice | 12 |

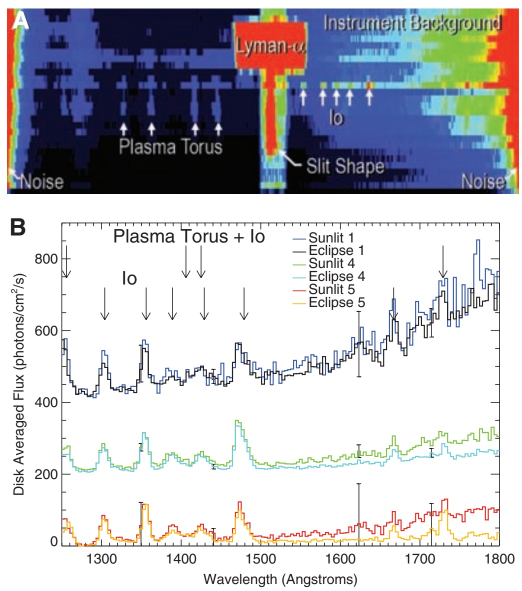


**Fig. 1.** (**A**) Alice spectral image, a combination of all IEclipse04 data. Features include Io in row 17, the Io plasma torus in rows 9 to 22, background interplanetary Lyman-α emissions in rows 7 to 26 (red rectangle/T-shaped slit; near this the sensitivity changes abruptly from a gap in the detector photocathode coverage), and increased detector noise at the left and right edges. Instrument-scattered Lyman-α from Jupiter and/or detector dark signal is ubiquitous at longer wavelengths in all rows and hint at row-to-row flat-field variations known from lab measurements. (**B**) Alice IEclipse01, IEclipse04, and IEclipse05 Io spectra combined into sunlit and eclipse averages. Spectra for each visit are offset by increments of 200 for clarity. Neutral and ionized atomic emissions are indicated with arrows ("Io" and "Plasma Torus + Io," respectively). The time variability is presented in Fig. 3, and integrated emission line brightnesses are listed in Table 2. Error bars are SDs of the variability. Adjacent rows are averaged for the background subtraction, which is incomplete at longer wavelengths.

[1]Southwest Research Institute, San Antonio, TX 78228, USA. [2]Southwest Research Institute, Boulder, CO 80302, USA. [3]NASA Headquarters, Washington, DC 20546, USA. [4]University of Cologne, 50923 Koln, Germany. [5]The Johns Hopkins University, Baltimore, MD 21218, USA. [6]The Johns Hopkins University Applied Physics Laboratory, Laurel, MD 20723, USA. [7]University of Colorado, Boulder, CO 80302, USA. [8]Jet Propulsion Laboratory, Pasadena, CA 91109, USA. [9]NASA Goddard Spaceflight Center, Greenbelt, MD 20771, USA. [10]NASA Ames Research Center, Moffett Field, CA 94035, USA.

*To whom correspondence should be addressed. E-mail: KRetherford@swri.edu

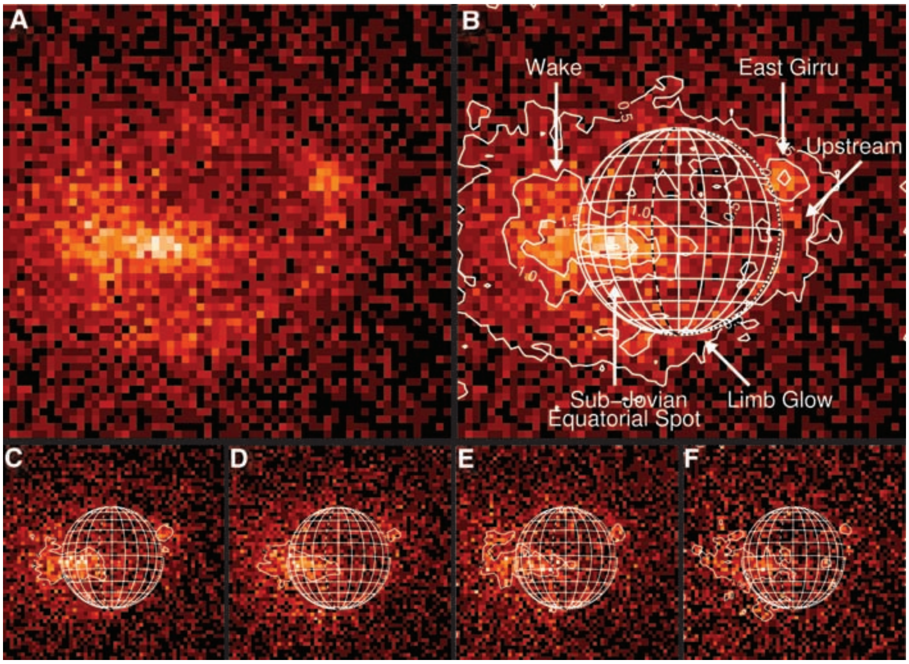


**Fig. 2.** HST/SBC FUV images of Io on 27 February 2007, concurrent with NH IEclipse03 observations. (**A**) Average of all eight 5-min HST exposures. (**B**) Same as (A), with labeled features. The sub-Earth longitude is 344°. The sub-jovian (0°) and orbital trailing (270°) longitudes are indicated with dashed and dotted meridians, respectively, with 15° gridding for the graticule. The view of Io from Earth is 33° from the concurrent NH view. Contours indicate 0.5 kilorayleigh (kR) increments in brightness levels. The aurora morphology is qualitatively consistent with previous FUV observations. The upstream-side auroral feature is nominally expected where the jovian magnetic field is tangent to the limb (shown with arrow). However, its location is ~15° North and likely influenced by the East Girru plume (*17*). The wake auroral feature is observed to extend >1 $R_{Io}$ downstream relative to the plasma flow. The 1.4 ± 0.1 times brighter southern polar limb glow measured between 0.75 and 1.25 $R_{Io}$ is consistent with Io being located "above" the plasma torus centrifugal equator (*23*). The nearby north, south, and west Masubi volcanoes known to be active at this time (*17*) may also enhance the southern limb glow brightness on the left (fig. S2). The F125LP filter includes FUV emissions in the 125-nm to 200-nm band-pass, which are primarily OI 130.4 nm, OI 135.6 nm, SI 138.9 nm, SI 147.9 nm, SI 166.7 nm, SI 181.2 nm, and SI 190.0 lines for atomic gas, with smaller contributions from ionized SII 125.6 nm, SII 142.9 nm, and SII 172.9 nm (*20*). (**C** to **F**) HST/SBC time series of 10-min (two exposure) averages. The brightness contours (labeled in kilorayleighs) are scaled to match the ~50% brightness level in each image to better compare the equatorial spot shape and latitudinal extent as a function of time. The latitudinal extent decreases by ~25% from (C) to (F).

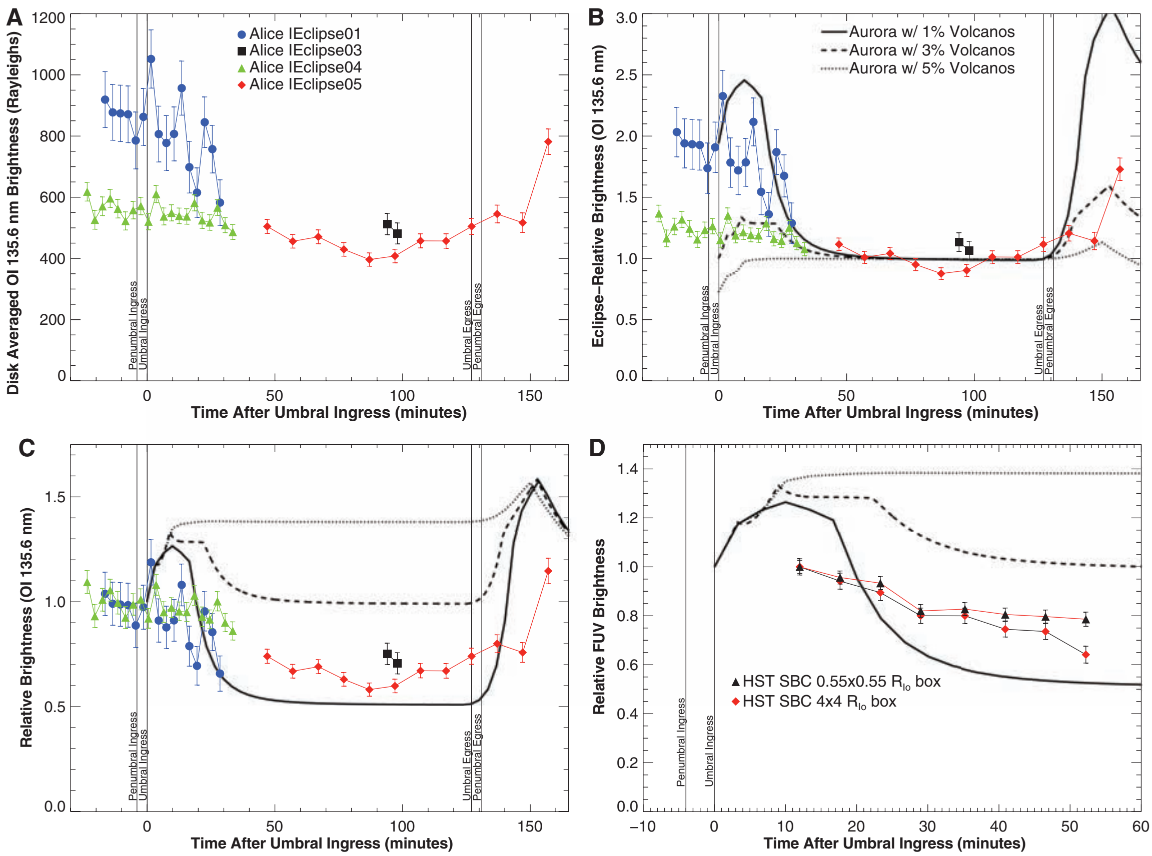


**Fig. 3.** Time series of Io's auroral emissions in Eclipse. (**A**) NH Alice IEclipse01, IEclipse03, IEclipse04, and IEclipse05 brightness measurements of OI 135.6 nm emissions are shown with time after umbral eclipse ingress. (**B**) Same as (A), but normalized to values in eclipse from 50 to 125 min after ingress and compared with aurora simulations (*14*) for three levels of volcanic contribution. (**C**) Same as (A) and (B), but normalized to pre-ingress, sunlit values. The last measurement in IEclipse05 supports the predicted posteclipse brightening. IEclipse01 views the dayside, whereas IEclipse04 views mostly the nightside and is dimmer. These diurnal (phase angle) variations indicate that the atmosphere in shadow (both on the nightside and in eclipse) is supplied primarily by volcanoes (see additional plots in fig. S1). IEclipse01, obtained at roughly twice the distance from NH as IEclipse04, has more statistical noise. (**D**) HST/ACS/SBC brightness measurements of regions within the limb and extending a few $R_{Io}$ with time in eclipse, concurrent with the IEclipse03 event. The SBC brightnesses decreased by a factor of 1.3 during the period between 20 min and 50 min after ingress.

**Table 2.** Alice-measured emission line brightness averages and SDs in sunlight and eclipse.

| Emission line | Type | Disk-average brightness (rayleighs) | | |
|---|---|---|---|---|
| | | IEclipse01 | IEclipse04 | IEclipse05 |
| **OI 130.4 nm** | Sunlight | 706 ± 134 | 445 ± 27 | 347 ± 142 |
| | Eclipse | 597 ± 43 | 394 ± 14 | 254 ± 71 |
| | Ratio S/E | 1.18 ± 0.24 | 1.12 ± 0.08 | 1.37 ± 0.68 |
| **OI 135.6 nm** | Sunlight | 882 ± 177 | 577 ± 35 | 480 ± 188 |
| | Eclipse | 797 ± 57 | 536 ± 18 | 381 ± 94 |
| | Ratio S/E | 1.11 ± 0.24 | 1.08 ± 0.08 | 1.26 ± 0.58 |
| **SI 147.9 nm** | Sunlight | 1167 ± 271 | 986 ± 54 | 596 ± 288 |
| | Eclipse | 1205 ± 87 | 874 ± 28 | 429 ± 144 |
| | Ratio S/E | 0.97 ± 0.24 | 1.13 ± 0.07 | 1.39 ± 0.82 |

NH Long Range Reconnaissance Imager (LORRI) images (*17*). This same feature appears in the HST/SBC image in Fig. 2B, obtained when East Girru was shifted just behind the limb. The auroral feature near East Girru in both LORRI and HST/SBC images is ~15° northward of Jupiter's field line tangent point at the limb, which suggests that ionospheric currents are diverted northward from this nominal position toward a region of higher gas density near the plume. Similar deviations of the anti-jovian FUV emissions from nominal tangent points observed with STIS are likely caused by the prevalence and distribution of plumes there (*21*). Volcanic plume aurorae were not identified in previous lower-quality STIS FUV images, which caused an apparent discrepancy with visible images of plume aurorae. The East Girru plume FUV auroral feature in Fig. 2 resolves this discrepancy and reveals the influence of plumes on Io's electrodynamic interaction. The upstream-side emission feature is more apparent when limb brightened at viewing geometries like those reported in Fig. 2. This feature was predicted by aurora image simulations (*22*) and is diagnostic of the divergence of the plasma flow upstream of Io, a primary trait of Io's interaction with the plasma torus.

### References and Notes


1. F. Bagenal, *J. Atmos. Sol. Terres. Phys.* **69**, 387 (2007).
2. E. Lellouch, M. A. McGrath, K. L. Jessup, in *Io After Galileo* (Springer-Praxis, UK, 2006), pp. 231–264.
3. J. Pearl *et al.*, *Nature* **280**, 755 (1979).
4. W. M. Sinton, C. Kaminski, *Icarus* **75**, 207 (1988).
5. J. R. Spencer *et al.*, *Science* **288**, 1198 (2000).
6. A. F. Cook *et al.*, *Science* **211**, 1419 (1981).
7. J. T. Clarke, J. Ajello, J. Luhmann, N. M. Schneider, I. Kanik, *J. Geophys. Res.* **99**, 8387 (1994).
8. P. E. Geissler *et al.*, *Science* **285**, 870 (1999).
9. A. H. Bouchez, M. E. Brown, N. M. Schneider, *Icarus* **148**, 316 (2000).
10. P. E. Geissler *et al.*, *J. Geophys. Res.* **106**, 26137 (2001).
11. P. E. Geissler *et al.*, *Icarus* **172**, 127 (2004).
12. I. DePater *et al.*, *Icarus* **156**, 296 (2002).
13. K. D. Retherford, thesis, The Johns Hopkins University (2002).
14. J. Saur, D. F. Strobel, *Icarus* **171**, 411 (2004).
15. S. A. Stern *et al.*, in *Astrobiology and Planetary Missions*, R. B. Hoover, G. V. Levin, A. Y. Rozanov, G. R. Gladstone, Eds. (Proc. SPIE, Volume 5906, 2005), pp. 358–367.
16. K. D. Retherford *et al.*, paper presented at the Magnetospheres of the Outer Planets Meeting, San Antonio, TX, 25 June, 2007.
17. J. R. Spencer *et al.*, *Science* **318**, 240 (2007).
18. The angular size of Io varies with spacecraft distance but is smaller than the Alice slit width for these data. The spectral resolution varies between 0.3 nm and ~0.9 nm for emissions known to be located near the satellite disk (*22*); see, e.g., Fig. 2.
19. H. C. Ford *et al.*, in *Future EUV/UV and Visible Space Astrophysics Missions and Instrumentation*, J. C. Blades, O. H. W. Siegmund, Eds. (Proc. SPIE, Volume 4854, 2003), pp. 81–94.
20. F. L. Roesler *et al.*, *Science* **283**, 353 (1999).
21. K. D. Retherford *et al.*, *J. Geophys. Res.* **105**, 27157 (2000).
22. J. Saur, F. M. Neubauer, D. F. Strobel, M. E. Summers, *Geophys. Res. Lett.* **27**, 2893 (2000).
23. K. D. Retherford, H. W. Moos, D. F. Strobel, *J. Geophys. Res.* **108**, 1333 (2003).
24. L. M. Feaga, thesis, The Johns Hopkins University (2005).
25. K. L. Jessup *et al.*, *Icarus* **169**, 197 (2004).
26. J. R. Spencer *et al.*, *Icarus* **176**, 283 (2005).
27. P. D. Feldman *et al.*, *Geophys. Res. Lett.* **27**, 1787 (2000).
28. D. F. Strobel, B. C. Wolven, *Astrophys. Space Sci.* **277**, 271 (2001).
29. F. Neubauer, *J. Geophys. Res.* **103**, 19843 (1998).
30. F. M. Neubauer, *J. Geophys. Res.* **104**, 3863 (1999).


31. We thank the New Horizons mission and science teams. New Horizons is funded by NASA. Support for this work was also provided by NASA though grant number GO-10871 from the Space Telescope Science Institute (STScI), which is operated by the Association of Universities for Research in Astronomy, Inc., under NASA contract NAS5-26555.


**Supporting Online Material**

www.sciencemag.org/cgi/content/full/318/5848/237/DC1
Figs. S1 and S2
Tables S1 and S2

10 July 2007; accepted 19 September 2007
10.1126/science.1147594



REPORT

# Io Volcanism Seen by New Horizons: A Major Eruption of the Tvashtar Volcano

J. R. Spencer,[1*] S. A. Stern,[2] A. F. Cheng,[2] H. A. Weaver,[3] D. C. Reuter,[4] K. Retherford,[5] A. Lunsford,[4] J. M. Moore,[6] O. Abramov,[1] R. M. C. Lopes,[7] J. E. Perry,[8] L. Kamp,[7] M. Showalter,[9] K. L. Jessup,[1] F. Marchis,[9] P. M. Schenk,[10] C. Dumas[11]

Jupiter's moon Io is known to host active volcanoes. In February and March 2007, the New Horizons spacecraft obtained a global snapshot of Io's volcanism. A 350-kilometer-high volcanic plume was seen to emanate from the Tvashtar volcano (62°N, 122°W), and its motion was observed. The plume's morphology and dynamics support nonballistic models of large Io plumes and also suggest that most visible plume particles condensed within the plume rather than being ejected from the source. In images taken in Jupiter eclipse, nonthermal visible-wavelength emission was seen from individual volcanoes near Io's sub-Jupiter and anti-Jupiter points. Near-infrared emission from the brightest volcanoes indicates minimum magma temperatures in the 1150- to 1335-kelvin range, consistent with basaltic composition.

The New Horizons (NH) Jupiter flyby provided the first close-up observations of the tidally driven volcanism of Jupiter's moon Io since the last Galileo orbiter observations of Io in late 2001 (*1*). The closest approach to Io occurred at 21:57 UT on 28 February 2007 at a range of 2.24 million km. Sunlit observations were made at solar phase angles from 5° to 159°, and four eclipses of Io by Jupiter were also observed. NH obtained 190 Io images with its 4.96 μrad per pixel panchromatic (400 to 900 nm) Long-Range Reconnaissance Imager (LORRI) and 17 color nighttime and eclipse images with the 20 μrad per pixel Multicolor Visible Imaging Camera (MVIC), although MVIC coverage of Io's day side was not possible because of detector saturation. NH also obtained seven 1.25- to 2.5-μm near-infrared image cubes at 62 μrad per pixel with the Linear Etalon Infrared Spectral Array instrument (LEISA) and numerous disk-integrated ultraviolet observations with the Alice instrument, discussed separately (*2*).

Eleven volcanic plumes were identified in the NH images (Fig. 1A and table S1). In addition to the single very large "Pele-type" plume at Tvashtar, which is described separately, NH observed 10 $SO_2$-rich "Prometheus-type" plumes (*3*–*5*). These smaller plumes averaged 80 km high and varied greatly in brightness. Plumes seen for the first time by NH include those at Zal and Kurdalagon and a large new plume, 150 km high, at north Lerna Regio, which has produced a large albedo change. Three of these plumes, north Lerna and north and south Masubi, are associated with recent large lava flows, supporting the idea that Prometheus-type plumes result from mobilization of surface volatiles by active lava flows. All active plumes that were on